

Wide-range coupling between surface plasmon polariton and cylindrical dielectric waveguide mode

Van Duong Ta, Rui Chen, and Han Dong Sun*

*Division of Physics and Applied Physics, School of Physical and Mathematical Sciences,
Nanyang Technological University, Singapore 637371, Singapore*

*hdsun@ntu.edu.sg

Abstract: A modified hybrid waveguide with a wide-range coupling and long propagation has been proposed and the coupled mode theory has been applied to study the hybrid waveguide systematically. Two structures are comparatively discussed, namely, a dielectric wire and a circular capillary tube, which are buried in a polymer matrix and separated from the silver substrate by a gap. The simulated results indicate that the circular capillary tube demonstrates a stronger coupling between the surface plasmon polariton and the waveguide mode compared to the solid dielectric wire. Furthermore, the electric field is highly confined in the gap area and can propagate several hundred micrometers.

© 2011 Optical Society of America

OCIS Codes: (230.7370) Waveguides; (240.6680) Surface plasmons.

References and links

1. R. Kirchain and L. Kimerling, "A roadmap for nanophotonics," *Nat. Photonics* **1**(6), 303–305 (2007).
2. C. Z. Ning, "Semiconductor nanolasers," *Phys. Status Solidi B* **247**, 774–788 (2010).
3. R. F. Oulton, V. J. Sorger, D. A. Genov, D. F. P. Pile, and X. Zhang, "A hybrid plasmonic waveguide for subwavelength confinement and long-range propagation," *Nat. Photonics* **2**(8), 496–500 (2008).
4. S. A. Maier, "Waveguiding—the best of both worlds," *Nat. Photonics* **2**(8), 460–461 (2008).
5. R. F. Oulton, V. J. Sorger, T. Zentgraf, R.-M. Ma, C. Gladden, L. Dai, G. Bartal, and X. Zhang, "Plasmon lasers at deep subwavelength scale," *Nature* **461**(7264), 629–632 (2009).
6. M. Z. Alam, J. Meier, J. S. Aitchison, and M. Mojahedi, "Propagation characteristics of hybrid modes supported by metal-low-high index waveguides and bends," *Opt. Express* **18**(12), 12971–12979 (2010).
7. I. Avrutsky, R. Soref, and W. Buchwald, "Sub-wavelength plasmonic modes in a conductor-gap-dielectric system with a nanoscale gap," *Opt. Express* **18**(1), 348–363 (2010).
8. Y. F. Xiao, B. B. Li, X. Jiang, X. Y. Hu, Y. Li, and Q. H. Gong, "High quality factor, small mode volume, ring-type plasmonic microresonator on a silver chip," *J. Phys. At. Mol. Opt. Phys.* **43**(3), 035402 (2010).
9. D. R. Chen, "Cylindrical hybrid plasmonic waveguide for subwavelength confinement of light," *Appl. Opt.* **49**(36), 6868–6871 (2010).
10. Y. S. Bian, Z. Zheng, Y. Liu, J. S. Zhu, and T. Zhou, "Dielectric-loaded surface plasmon polariton waveguide with a holey ridge for propagation-loss reduction and subwavelength mode confinement," *Opt. Express* **18**(23), 23756–23762 (2010).
11. D. K. Gramotnev and S. I. Bozhevolnyi, "Plasmonics beyond the diffraction limit," *Nat. Photonics* **4**(2), 83–91 (2010).
12. H. J. Moon, G. W. Park, S. B. Lee, K. An, and J. H. Lee, "Waveguide mode lasing via evanescent-wave-coupled gain from a thin cylindrical shell resonator," *Appl. Phys. Lett.* **84**(22), 4547–4549 (2004).
13. G. Ghosh, "Dispersion-equation coefficients for the refractive index and birefringence of calcite and quartz crystals," *Opt. Commun.* **163**(1-3), 95–102 (1999).
14. P. B. Johnson and R. W. Christy, "Optical constants of the noble metals," *Phys. Rev. B* **6**(12), 4370–4379 (1972).
15. W. L. Barnes, A. Dereux, and T. W. Ebbesen, "Surface plasmon subwavelength optics," *Nature* **424**(6950), 824–830 (2003).

1. Introduction

Manipulating laser sources in micrometer and nanometer scale is significant because they are essential components in photonic integrated circuits [1,2]. Recently, the combination of

surface plasmon polaritons (SPP) and dielectric waveguide (DW) to form the so-called hybrid plasmonic waveguide has been demonstrated successfully [3]. In this hybrid configuration, electromagnetic field is highly confined in the gap area which can propagate several hundred micrometers. Therefore, the hybrid SPP waveguide shows high confinement and low transmission loss, which points to a new approach to manipulating nanophotonic devices [3,4]. Based on this idea, a plasmonic laser at deep subwavelength scale has been reported [5], and research down this line has drawn considerable attention. Various dielectric-gap-metal structures such as nanowire [3], slab [6,7], ring-type [8], cylindrical core-shell [9] and dielectric-loaded [10] have been proposed and discussed.

However, it is found that for all the reported models, the gap width (h) between SPP and DW should be in nanoscale [3,6–10]. For instance, when the gap is larger than 100 nm, the interaction between the two modes is rather weak, especially for the nanowire with large diameter [3]. This limitation unavoidably imposes critical influence on the hybrid mode quality, especially when the nanowire has structure imperfection such as surface roughness and shape non-uniformities [11]. Consequently, a new scheme which is flexible and less sensitive to both the gap and the diameter is desirable.

In this work, we propose and numerically analyze an alternative model which shows attractive advantages over the traditional ones. The idea is based on a circular capillary tube (CCT) [12] in micrometer size. Simulation results show that the coupling in the proposed structure preserves for a wide-range of h . This approach boosts the feasibility of hybrid waveguide between SPP and DW in micro-scale, and therefore contributes to improve the quality and reliability of micro- and nanolasers.

2. Model and theory

The two structures discussed herein are schematically drawn in Fig. 1. The traditional model is presented in Fig. 1(a), which consists of a 3 μm diameter silicon dioxide (SiO_2) microwire (refractive index $n_o = 1.53$ in the telecommunication wavelength $\lambda = 1550$ nm) [13] buried in a chemical stable polydimethylsiloxane polymer (PDMS) matrix with lower refractive index ($n_p = 1.41$) [8]. The wire is held parallel above the silver surface with refractive index $n_m = 0.145 + 13.26i$ by a gap h [14]. The same structure is applied to the proposed model except that the wire is replaced by the CCT. The outer diameter of the CCT is the same with the first case (3 μm), and the inner hole diameter is D , which is filled with air. As is well-known, the electromagnetic energy is confined in the region with high permittivity as shown in Fig. 1 [3,12]. It can be seen that the mode field distribution in the CCT is closer to the metal surface despite of the same h above the metal surface. It is therefore expected that the interaction between SPPs and DW should be stronger in the proposed structure.

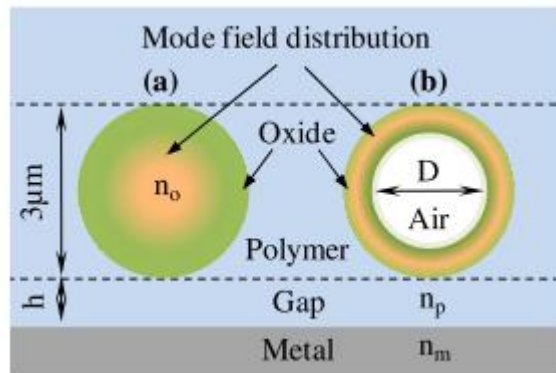


Fig. 1. Schematic diagram of the hybrid waveguides. (a) The conventional and (b) the proposed structure.

The coupled mode theory was applied to study the dependence of hybrid waveguide mode on both inner diameter D of the CCT and gap width h in the telecommunication wavelength [3]. In this theory, the hybrid mode is the result of a linear “superposition” of two pure separated waveguide modes: the CCT (cylinder modes) without metallic region and the SPP modes without CCT by the following equation [3],

$$\psi_{hyb}(D,h) = a(D,h)\psi_{cct}(D) + b(D,h)\psi_{spp} \quad (1)$$

where $\psi_{cct}(D)$ and ψ_{spp} are the basis mode of CCT and SPP, respectively. $a(D,h)$ and $b(D,h)$ are the amplitude of each component. By means of the finite element method (FEM) supported by COMSOL Multiphysics, numerical data can be obtained for later discussion.

3. Results and discussion

Figure 2 plots the calculated electric energy density of hybrid modes for the two cases. In the traditional model, the electromagnetic field is not fully confined in the gap region for small h (such as $h = 30$ nm) but spreads to wide range of the wire body as shown in Fig. 2(a). In addition, the interaction drops quickly with the increase of h . For example, if $h = 200$ nm, the hybrid mode is nearly pure cylinder mode [Fig. 2(b)], and there is almost no interaction for $h = 400$ nm [Fig. 2(c)]. These results obviously exhibit the disadvantage of the conventional configuration that the coupling between SPP and DW is very sensitive to the gap width.

However, the results are totally different for the proposed structure. It can be seen that the interaction is strong for small gap width $h = 30$ nm as shown in Fig. 2(d). Most of the energy is strongly trapped in the gap region. The interaction is still strong when h rises to 200 nm [Fig. 2(e)] and remains moderately strong for $h = 400$ nm [Fig. 2(f)]. Interestingly, for large h , the electric field energy is highly focused in the gap instead of oxide region. Therefore, it provides a good medium for studying light-matter interaction inside the gap area. Evidently, the coupling in our model does not sensitively depend on h . The obtained results remarkably improve the coupling range, which verifies our prediction.

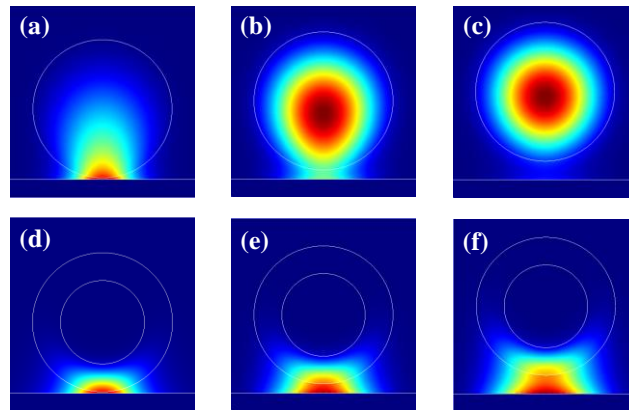


Fig. 2. Calculated electric energy density of hybrid modes. (a), (b), (c) The traditional model for different gap widths $h = 30, 200, 400$ nm, respectively. (d), (e), (f) The proposed model with the same parameters and the inner diameter $D = 1.8 \mu\text{m}$.

To better understand the coupling ability, electric energy density of the hybrid mode along the vertical direction is extracted and plotted in Fig. 3. The results indicate that the energy density is higher in the gap area and decreases with increasing h . This is understandable because the energy density reduces due to the expanding of gap area, which is proportional to h .

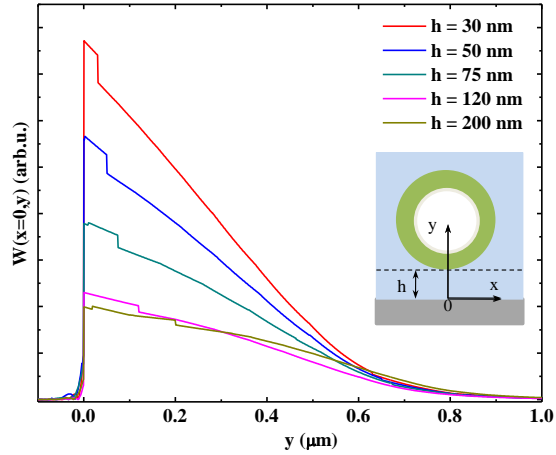


Fig. 3. Electric energy density of the hybrid mode along y direction ($x = 0$) of the proposed mode in the case of $D = 1.8 \mu\text{m}$ as a function of h

One requirement of strong coupling between SPPs and DW is that the real parts of their complex eigenvalues, called effective index, should be the same. For better understanding, we analyze the effective index and mode character of the hybrid mode as a function of h and D as shown in Fig. 4. It can be clearly seen in Fig. 4(a) that the change of effective index of hybrid mode in all cases is tiny. The maximum is 1.49 while the minimum is approximately 1.425, which is slightly dependent on both h and D . It is found that for the same D , the effective index of the hybrid mode increases for smaller h . Moreover, the effective index of pure cylinder mode decreases as D increases. This should be understandable because for small D , like $1 \mu\text{m}$, the thickness of the oxide is large and mode field is highly confined in oxide area. Therefore the effective index of the waveguide should be close to the refractive index of the oxide ($n_o = 1.53$). In contrast, for larger D the oxide thickness becomes thinner and the waveguide mode expands to polymer area so the effective refractive index of the waveguide drops and approaches to the refractive index of the polymer ($n_p = 1.41$). This is the reason why the effective index of the dielectric waveguide drops with increasing h and D . The mode character of hybrid mode is defined by square of the coefficients $a(D, h)$ or $b(D, h)$, for instance [3],

$$a(D, h)^2 = \frac{n_{\text{hyb}}(D, h) - n_{\text{spp}}}{n_{\text{hyb}}(D, h) - n_{\text{cct}}(D) + n_{\text{hyb}}(D, h) - n_{\text{spp}}} \quad (2)$$

where $n_{\text{spp}} = \sqrt{\varepsilon_m \varepsilon_p / (\varepsilon_m + \varepsilon_p)}$ and $n_{\text{cct}}(D)$ is the effective index of CCT waveguide mode as a function of D . Based on this definition, the mode is cylinder-like if $a(D, h)^2 < 0.5$ and SPP-like if $a(D, h)^2 > 0.5$ [3]. When $a(D, h)^2 = 0.5$ the coupling is the strongest, which corresponds to half SPP and half cylindrical waveguide. As depicted in Fig. 4(b), the mode character shows a slight change from 0.7 to 0.4 for $h = 30 \text{ nm}$ and bigger change from 0.9 to 0.25 (but not from 1 to 0) for $h = 400 \text{ nm}$ when D increase from 1 to 2 μm , respectively. The strongest coupling appears when $D = 1.78 \mu\text{m}$.

The propagation distance characterizes transmission loss of the hybrid waveguide which can be found from the imaginary part of complex hybrid wave vector along the propagation direction, $k_{\text{hyb}}(D, h)$ [3,15],

$$L_p = 1 / (2 \text{Im}[k_{\text{hyb}}(D, h)]) \quad (3)$$

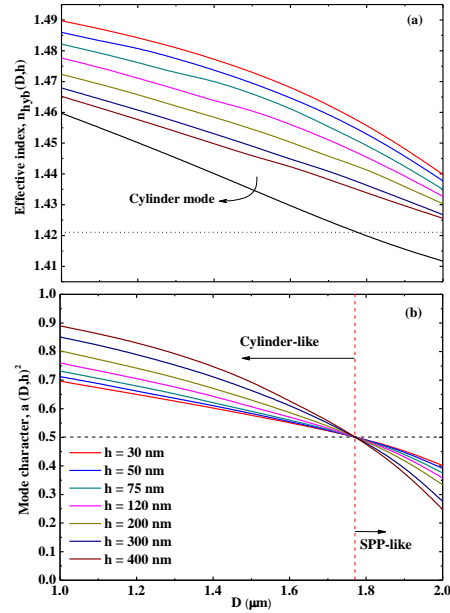


Fig. 4. (a) The effective index and (b) the mode character of hybrid mode for different h compared with pure cylinder mode and SPP mode of metal – polymer (dotted line). The vertical red dashed line denotes the strong coupling regime.

Figure 5 shows dependence of the propagation length on h and D , respectively. The propagation length of hybrid mode in the strongest section ranges from about 240 μm for $h = 30$ nm to 540 μm for $h = 400$ nm (Fig. 5). When the gap is larger than 300 nm, the propagation distance exceeds its two pure SPP modes: metal-oxide (SPP1) and metal-polymer (SPP2). The value is comparable to SPP modes when h is around 200 nm and smaller in the conventional case. Obviously, the propagation distance is controllable by changing the gap width.

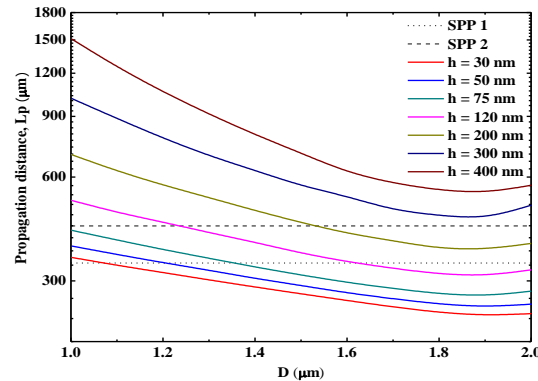


Fig. 5. Propagation distance of the hybrid mode compared with two pure SPP modes: metal-oxide (SPP1) and metal-polymer (SPP2).

For the proposed model structure, the coupling width can be as large as 400 nm, and the propagation distance is several hundred micrometers and the electric field is highly focused on the gap area. Thus, the model structure provides a good cavity for laser observation if an active gain material is located in the gap area. Therefore, this new approach is important for high efficiency micro- and nanolasers. In addition, the high electric energy density in the gap

region may support fundamental studies such as light and matter interaction and nonlinear optical phenomena.

A proposed fabrication process may be as following. First, the silver thin film, which is up to 100nm, can be deposited on a substrate by electron beam evaporation. Subsequently, a solution of PDMS in some proper organic solvent, such as, chloroform, ether or tetrahydrofuran (THF) is directly deposited on top of the thin film by spin coating. The thickness of polymer is controllable, which depends on angular frequency of spin coater and viscosity of the solution. After that, the sample is exposed to the air for several hours before additionally cured in an oven with high temperature. This treatment helps to evaporate the solvent and make the polymer film more stable. The CCT is then carefully put on the polymer surface. In the final process, a droplet of pure PMDS (liquid form) is dropped on the structure to complete the sample.

4. Conclusion

In summary, the CCT has been proposed for the advantageous hybrid waveguide structure. The proposed structure can enlarge the coupling width significantly, which leads to wider range coupling between SPPs and DW. The simulated results indicate that the coupling is practically stable with the change of both h and D . This is advantageous in suppressing the adverse influence caused by the structural imperfection. The investigation has demonstrated the superiorities of hybrid structures, and is important to develop plasmonic micro- and nanolasers.

Acknowledgment

Support from the Singapore Ministry of Education through the Academic Research Fund (Tier 1) under Project No. RG63/10 is gratefully acknowledged.